The following Communications have been judged by at least two referees to be "very important papers" and will be published online at www.angewandte.org soon:

M. Mascal, E. B. Nikitin*
Direct, High-Yield Conversion of Cellulose into Biofuel

P. García-Álvarez, D. V. Graham, E. Hevia, A. R. Kennedy, J. Klett, R. E. Mulvey, C. T. O Hara, S. Weatherstone*
Unmasking Representative Structures of TMP-Active Hauser and Turbo Hauser Bases

D. Staack, A. Fridman, A. Gutsol, Y. Gogotsi, G. Friedman**
Nanoscale Corona Discharge in Liquids Enabling Nanosecond Optical Emission Spectroscopy

*C. Hawner, K. Li, V. Cirriez, A. Alexakis**
Copper-Catalyzed Asymmetric Conjugate Addition of Aryl Aluminum Reagents to Trisubstituted Enones: Construction of Aryl-Substituted Quaternary Centers

*K. W. Eberhardt, C. L. Degen, A. Hunkeler, B. H. Meier**
One- and Two-Dimensional NMR Spectroscopy with a Magnetic-Resonance Force Microscope

*S. Wan, J. Guo, J. Kim, H. Ihee, D. Jiang**
A Belt-Shaped, Blue-Luminescent and Semiconducting Covalent Organic Framework

News

Books

Highlights

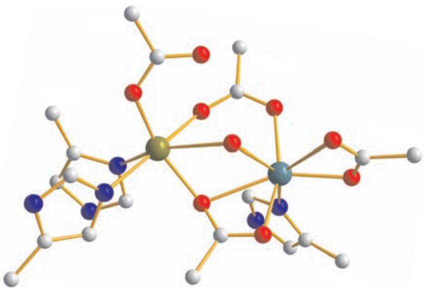

To mix or not to mix: The N-oxygenase AurF of *S. thioluteus* has an unusual carboxylate-bridged dinuclear active site (see picture; gray C, blue N, red O, green Mn, turquoise Mn/Fe). The similarity with a recently discovered Mn/Fe-oxygenase subunit of the ribonucleotide reductase of *C. trachomatis* suggests that it might contain both Mn and Fe. The N-oxygenase of *S. thioluteus* very likely represents the first member of a new family of Mn/Fe-oxygenases.

Bioinorganic Chemistry

Minireviews

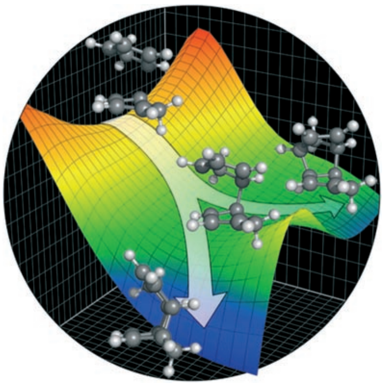

Path of least resistance: Reaction pathway bifurcations have been identified for many complex organic transformations. This type of potential energy surface describes a two-step-no-intermediate reaction mechanism that is neither stepwise nor concerted. Selective formation of one product over another is governed by the potential energy surface shape and resulting dynamic effects, not by transition state energetics.

Reaction Pathway Bifurcations

Reviews

Biosensors

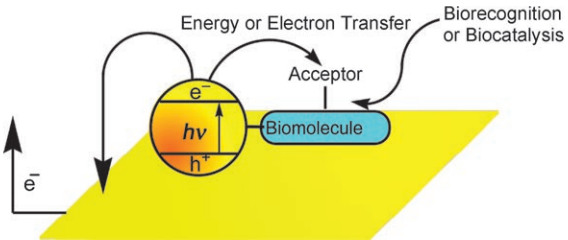

Hybrids of biomolecules and semiconductor quantum dots (QDs) are functional units for the optical, photoelectrochemical, and electrochemical analysis of biorecognition events or biocatalyzed transformations. The size-controlled fluorescence properties of QDs enable multiplexed bioanalysis, and by their coupling to appropriate quencher units, the optical probing of dynamic biocatalytic processes is feasible. The integration of electrodes into biomolecule–QD hybrids allows the measurement of biorecognition processes or transformations by photocurrents.

Communications

Peptide Recognition

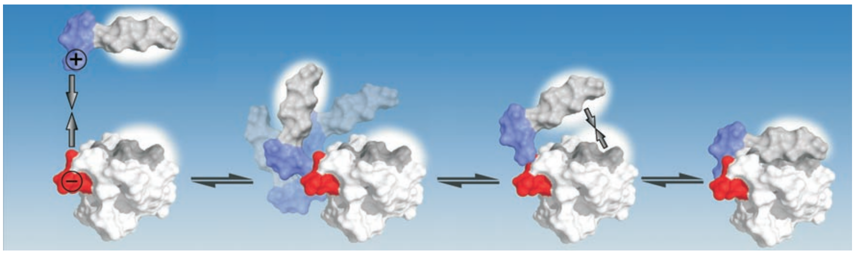

The complete pathway of the association of a proline-rich motif to an SH3 domain was probed by molecular dynamics simulations. The results indicate a bimodal binding mechanism, in which nature uses the reduction in dimensionality and hydrophobic dewetting as tools to find a simple solution to a seemingly complicated binding process.

Ionic Liquids (1)

Low melting, highly luminescent: [C$_3$mim][Eu(Tf$_2$N)$_4$] (**1**), [C$_4$mim][Eu(Tf$_2$N)$_4$], and [C$_4$mpyr]$_2$[Eu(Tf$_2$N)$_5$] are the first lanthanide ionic liquids that do not need stabilization of the liquid state by neutral coligands. They show excellent photophysical properties, such as long lifetimes of luminescence at large Eu^{III} concentration, small line width, and high color purity (see emission spectrum of **1** and photograph of a sample under UV light).

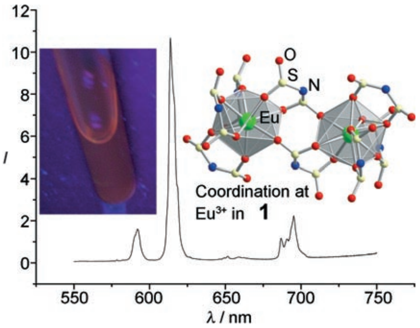

For the USA and Canada:
ANGEWANDTE CHEMIE International Edition (ISSN 1433-7851) is published weekly by Wiley-VCH, PO Box 191161, 69451 Weinheim, Germany. Air freight and mailing in the USA by Publications Expediting Inc., 200 Meacham Ave., Elmont, NY 11003. Periodicals postage paid at Jamaica, NY 11431. US POSTMASTER: send address changes to *Angewandte Chemie*, Wiley-VCH, 111 River Street, Hoboken, NJ 07030. Annual subscription price for institutions: US$ 7225/6568 (valid for print and electronic / print or electronic delivery); for individuals who are personal members of a national chemical society prices are available on request. Postage and handling charges included. All prices are subject to local VAT/ sales tax.

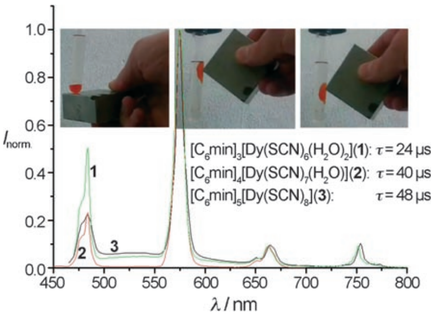

Attractive liquids: Dysprosium-based ionic liquids **1**–**3** show the highest response to external magnetic fields to date, allowing magnetic manipulation of the liquid (see pictures). At the same time, the liquids have excellent photophysical properties, such as long luminescence decay times τ and high color purity. The figure shows emission spectra of the ionic liquids.

Ionic Liquids (2)

B. Mallick, B. Balke, C. Felser, A.-V. Mudring* ______ **7635 – 7638**

Dysprosium Room-Temperature Ionic Liquids with Strong Luminescence and Response to Magnetic Fields

---

Shape control: Gold nanorods are synthesized in high yields in the absence of shape-regulating agents in 1-ethyl-3-methylimidazolium ethylsulfate ([EMIM][ES]). A two-step seeded-growth process is used that capitalizes on the binding affinity of imidazolium cations to gold crystal facets, the stabilization of Au^I in [EMIM][ES], and the reduction of particle growth rates that is facilitated by weak reducing agents.

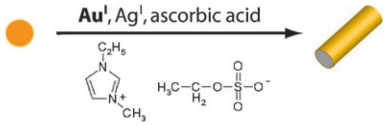

Anisotropic Nanoparticles

H. J. Ryu, L. Sanchez, H. A. Keul, A. Raj, M. R. Bockstaller* ______ **7639 – 7643**

Imidazolium-Based Ionic Liquids as Efficient Shape-Regulating Solvents for the Synthesis of Gold Nanorods

---

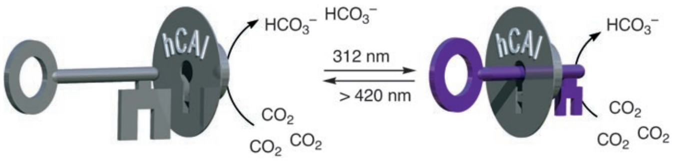

Photoswitchable: The activity of a dithienylethene-based human carbonic anhydrase inhibitor (hCAI) can be regulated using light. Converting the flexible, ring-open isomer of the photoswitch into the rigid, ring-closed isomer using UV light reduces the inhibition and increases the activity of hCAI by 50-fold. The inhibitor can be turned back on by using visible light, which has many advantages in biological applications.

Light-Regulated Enzyme Activity

D. Vomasta, C. Högner, N. R. Branda,* B. König* ______ **7644 – 7647**

Regulation of Human Carbonic Anhydrase I (hCAI) Activity by Using a Photochromic Inhibitor

---

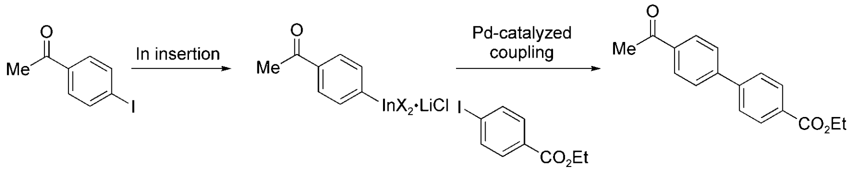

Sensitive functional groups, including ketone, aldehyde, and ester groups, may be present in aryl indium reagents prepared in good to excellent yields by the treatment of aryl and heteroaryl iodides with indium powder in the presence of LiCl (see example). These functionalized organoindium(III) reagents readily undergo Pd-catalyzed cross-coupling with functionalized aryl iodides, including those containing NH or OH groups.

Functionalized Indium Reagents

Y.-H. Chen, P. Knochel* ______ **7648 – 7651**

Preparation of Aryl and Heteroaryl Indium(III) Reagents by the Direct Insertion of Indium in the Presence of LiCl

The Barcelona® Chair by Knoll, Inc.

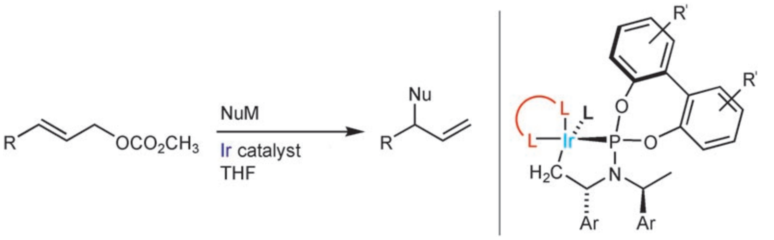

A final tweak: A new phosphoramidite iridium catalyst (see scheme) allows allylic substitutions to be run with a higher degree of regioselectivity than with other iridium catalysts and under aerobic conditions. Mechanistic aspects, in particular, the reversibility of the catalyst formation by C–H activation, are also presented. $\overset{\frown}{\mathrm{L\,L}}$ = dibenzocyclooctatetraene.

Allylic Substitution

S. Spiess, C. Welter, G. Franck,
J.-P. Taquet, G. Helmchen* **7652 – 7655**

Iridium-Catalyzed Asymmetric Allylic Substitutions—Very High Regioselectivity and Air Stability with a Catalyst Derived from Dibenzo[*a*,*e*]cyclooctatetraene and a Phosphoramidite

---

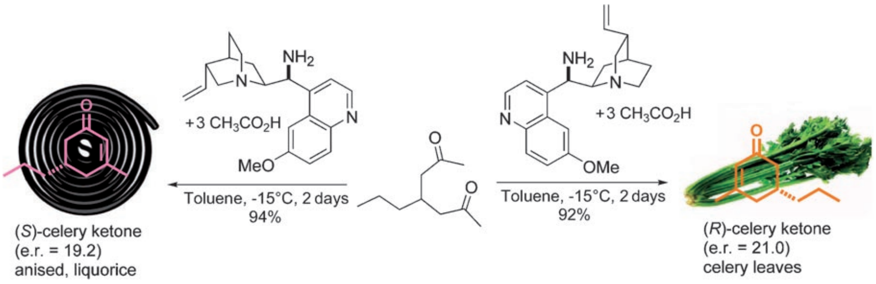

Aldol cyclodehydration of 4-substituted-2,6-heptanediones leads to enantiomerically enriched 5-substituted-3-methyl-2-cyclohexene-1-ones, which serve as perfume ingredients and valuable synthetic building blocks. Primary amines derived from cinchona alkaloids in combination with acetic acid are efficient catalysts for this transformation, which deliver both enantiomers of the celery ketone.

Organocatalysis

J. Zhou, V. Wakchaure, P. Kraft,
B. List* **7656 – 7658**

Primary-Amine-Catalyzed Enantioselective Intramolecular Aldolizations

---

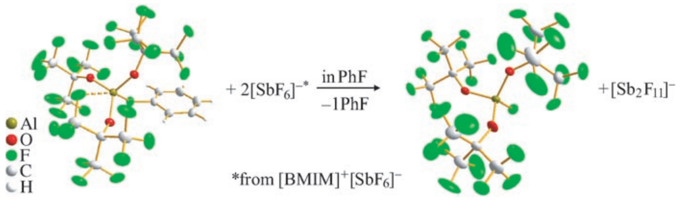

Lewis superacidity? In analogy to Brønsted superacids, Lewis superacids can be defined as Lewis acids that are stronger than the strongest conventional and commercially employed Lewis acid SbF_5. The fluorobenzene complex $PhF \rightarrow Al(OR^F)_3$ ($R^F = C(CF_3)_3$) qualifies as an easily accessible, non-oxidizing and stable Lewis acid that conforms with our Lewis superacidity criterion.

Lewis Superacids

L. O. Müller, D. Himmel, J. Stauffer,
G. Steinfeld, J. Slattery,
G. Santiso-Quiñones, V. Brecht,
I. Krossing* **7659 – 7663**

Simple Access to the Non-Oxidizing Lewis Superacid $PhF \rightarrow Al(OR^F)_3$ ($R^F = C(CF_3)_3$)

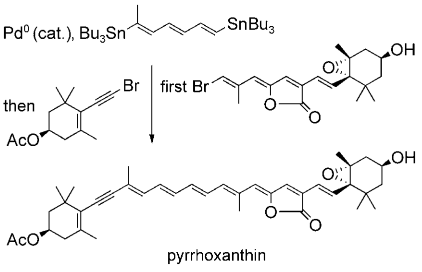

A carotenoid from the chemical kitchen: Two sequential Stille couplings of an unsymmetric distannane building block with a bromoolefin and a bromoalkyne terminated a highly convergent synthesis of the title compound, pyrrhoxanthin (see scheme).

Carotenoids

J. Burghart, R. Brückner* **7664 – 7668**

Total Synthesis of Naturally Configured Pyrrhoxanthin, a Carotenoid Butenolide from Plankton

Contents

Synthetic Methods

T. Gendrineau, O. Chuzel, H. Eijsberg, J.-P. Genet, S. Darses* ______ **7669 – 7672**

C_1-Symmetric Monosubstituted Chiral Diene Ligands in Asymmetric Rhodium-Catalyzed 1,4-Addition Reactions

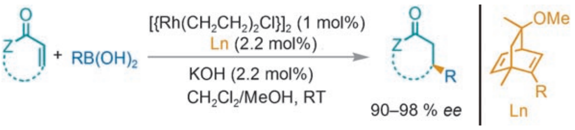

One trumps two: Monosubstituted chiral bicyclo[2.2.2]octadiene ligands, derived from carvone, form complexes with rhodium to catalyze the asymmetric addition of boronic acid substrates to α,β-unsaturated ketones (see scheme). The 1,4-adducts are produced in good yield and high enantioselectivity.

Synthetic Methods

S. Akai,* T. Ikawa, S. Takayanagi, Y. Morikawa, S. Mohri, M. Tsubakiyama, M. Egi, Y. Wada, Y. Kita ______ **7673 – 7676**

Synthesis of Biaryl Compounds through Three-Component Assembly: Ambidentate Effect of the *tert*-Butyldimethylsilyl Group for Regioselective Diels–Alder and Hiyama Coupling Reactions

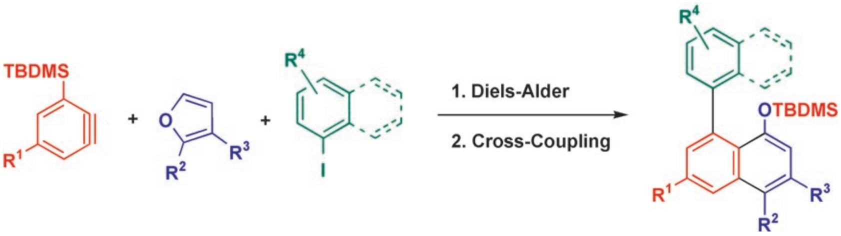

Two for the price of one: A method has been developed for the regiocontrolled synthesis of multisubstituted biaryl derivatives. This protocol involves the use of the *tert*-butyldimethylsilyl (TBDMS) group to direct the regioselective Diels–Alder reaction of a 3-TBDMS-benzyne with a furan derivative and a subsequent Hiyama cross-coupling reaction of the TBDMS group with aryl iodides (see scheme).

Quantum Dots

R. G. Xie, X. G. Peng* ______ **7677 – 7680**

Synthetic Scheme for High-Quality InAs Nanocrystals Based on Self-Focusing and One-Pot Synthesis of InAs-Based Core–Shell Nanocrystals

Paint by number: High-quality InAs quantum dots (QDs) for near-IR fluorescence (see picture) were synthesized by exploiting interparticle diffusion and self-focusing instead of using the traditional focusing of size distribution. InAs/CdSe core–shell QDs were grown and analyzed by a technique combining TEM and elemental analysis to determine the sizes and molar extinction coefficients of the extremely small InAs particles.

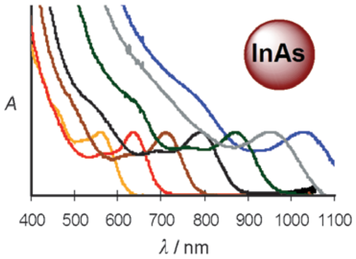

Nanostructures

S. Zhou, X. Liu, Y. Lin, D. Wang* ______ **7681 – 7684**

Spontaneous Growth of Highly Conductive Two-Dimensional Single-Crystalline $TiSi_2$ Nanonets

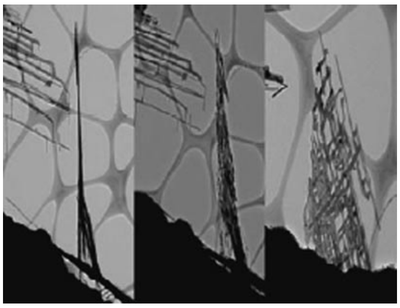

Net result: Two-dimensional nanonets form spontaneously in a chemical vapor deposition reaction. All beams in the nanonet are single-crystalline nanobelts that are connected by 90° joints. The nanonets are roughly 15 nm thick and a few micrometers long and wide (see pictures for three images at different tilting angles), and they assume a C49 $TiSi_2$ structure.

Magnetic Nanocups

D. Jagadeesan, U. Mansoori, P. Mandal, A. Sundaresan, M. Eswaramoorthy* ______ 7685 – 7688

Hollow Spheres to Nanocups: Tuning the Morphology and Magnetic Properties of Single-Crystalline α-Fe_2O_3 Nanostructures

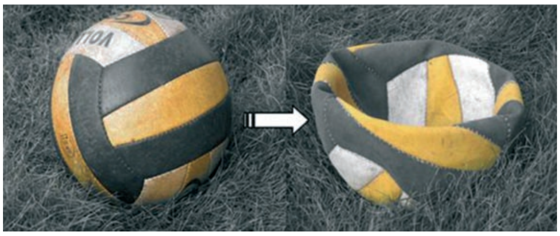

A bottom-up approach has been used to tune the morphology of single-crystalline hematite from hollow spheres to nanocups. The mechanism involves the formation of nanocups through buckling of the spheres, similar to a deflated ball (see picture). As the shape changes, there is a drastic change in magnetic properties.

Oxidative Methane Coupling

K. Takanabe, E. Iglesia* ______ 7689 – 7693

Rate and Selectivity Enhancements Mediated by OH Radicals in the Oxidative Coupling of Methane Catalyzed by $Mn/Na_2WO_4/SiO_2$

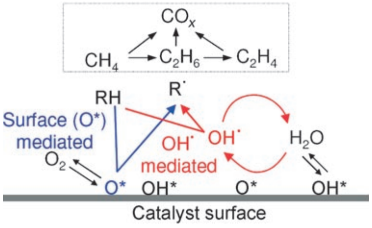

Radically Improved: OH radicals formed by quasi-equilibrated steps on oxide surfaces introduce homogeneous pathways that lead to higher rates and C_2 yields in oxidative methane coupling relative to those attained by CH_4 activation with chemisorbed oxygen (see picture; O*: dissociated oxygen atom; R: abstractor). The reactivity of OH˙ leads to a weaker influence of the C–H bond energies on the relative rates of H abstraction from CH_4, C_2H_6, and C_2H_4.

Olefin Hydroarylation

A. T. Luedtke, K. I. Goldberg* ______ 7694 – 7696

Intermolecular Hydroarylation of Unactivated Olefins Catalyzed by Homogeneous Platinum Complexes

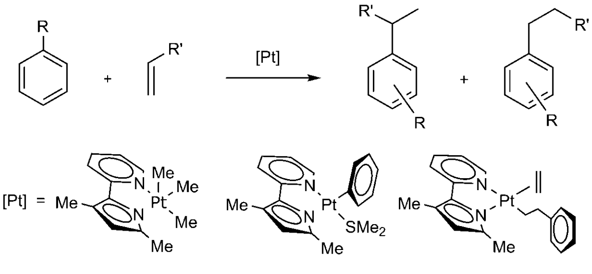

A **B** **C**

Designing catalysts: The five-coordinate platinum(IV) complex **A** and the platinum(II) *trans* complex **B** act as precatalysts for the hydroarylation of unactivated olefins. The catalytic cycle features an aryl–olefin insertion at Pt^{II} and a C–H bond activation of the arene solvent as key steps. The Pt^{II} *cis* complex **C** has been observed in hydroarylation reactions of ethylene with benzene.

Bioinorganic Chemistry

M. J. Zdilla, A. Q. Lee, M. M. Abu-Omar* ______ 7697 – 7700

Bioinspired Dismutation of Chlorite to Dioxygen and Chloride Catalyzed by a Water-Soluble Iron Porphyrin

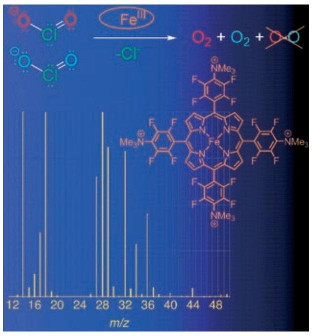

Cleaning up chlorite: A water-soluble iron porphyrin catalyzes the dismutation of chlorite to dioxygen and chloride. Labeling experiments demonstrate a novel mechanism for O=O bond formation. These mechanistic insights should aid in the design of catalysts for remediation of oxychlorine contaminants.

Hydrosilylation

A. Y. Khalimon, R. Simionescu, L. G. Kuzmina, J. A. K. Howard, G. I. Nikonov* ____ **7701 – 7704**

Agostic NSi–H⋯Mo Complexes: From Curiosity to Catalysis

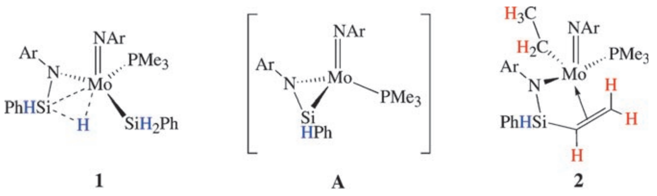

An uncommon catalyst: The β-agostic NSi–H⋯M complex **1** (Ar = 2,6-diisopropylphenyl) catalyzes a variety of hydrosilylation reactions. Stoichiometric reactions of **1** with unsaturated compounds proceed via the silanimine intermediate **A** and, in the case of olefins or nitriles, give products of Si–C coupling, such as **2**.

Molecular Codes

A. D. Shaller, W. Wang, H. Gan, A. D. Q. Li* ____ **7705 – 7709**

Tunable Molecular Assembly Codes Direct Reaction Pathways

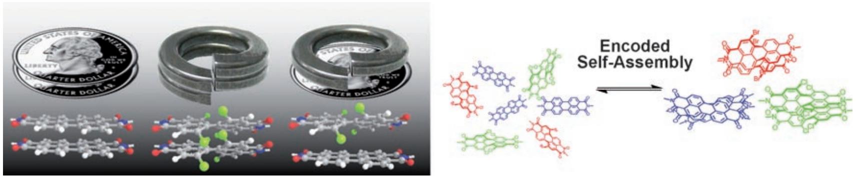

In the twist: The extent of twisting from planarity in a series of perylenetetracarboxylic diimides (PDIs) modulates the attractive π–π stacking force, revealing an array of inherent molecular recognition codes. Such coded self-assembly directs specific reaction pathways so that a mixture of reactive monomers with different codes results in identical products as when the reactions were carried out in separate flasks (see picture).

Organocatalysis

X. Lu, L. Deng* ____ **7710 – 7713**

Asymmetric Aza-Michael Reactions of α,β-Unsaturated Ketones with Bifunctional Organic Catalysts

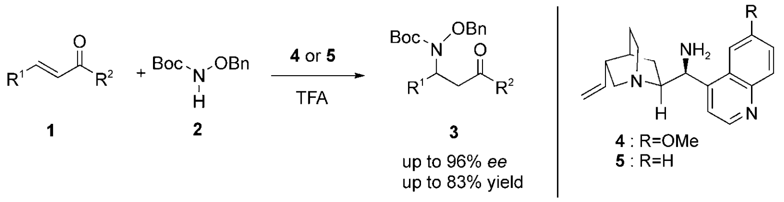

Synergy makes it possible: Bifunctional cinchona alkaloids are found to promote the first highly enantioselective organocatalytic aza-Michael reactions with α,β-unsaturated ketones. In addition to utilizing practical catalysts, readily accessible substrates, and commercially available reagents, this reaction affords a synthetically valuable scope that is complimentary to existing methods catalyzed by chiral metal complexes.

Asymmetric Catalysis

T. Mandal, C.-G. Zhao* ____ **7714 – 7717**

Modularly Designed Organocatalytic Assemblies for Direct Nitro-Michael Addition Reactions

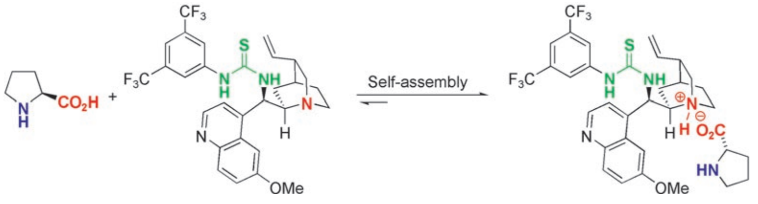

It's so simple! Organocatalysts formed through the self-assembly of simple α-amino acids and alkaloid thiourea derivatives (see scheme) are used as highly efficient catalysts for the direct nitro-Michael addition of ketones and nitroalkenes, affording excellent *ee* values up to 99%. Enantioselectivity may be tuned by changing components of the self-assembled catalyst.

Grignard Reagents

T. Robert, J. Velder,
H.-G. Schmalz* ____________ 7718 – 7721

Enantioselective Cu-Catalyzed 1,4-Addition of Grignard Reagents to Cyclohexenone Using Taddol-Derived Phosphine–Phosphite Ligands and 2-Methyl-THF as a Solvent

A small library of modular P,P ligands was screened and a potent Cu-based catalyst system was identified for highly enantioselective 1,4-additions to cyclohexenone with an unprecedented broad spectrum of Grignard reagents. Surprisingly, the highest selectivities were achieved in most cases in 2-methyl-THF, a “green” solvent underestimated so far.

Nanoscale Metal–Organic Frameworks

K. M. L. Taylor, A. Jin,
W. Lin* ____________ 7722 – 7725

Surfactant-Assisted Synthesis of Nanoscale Gadolinium Metal–Organic Frameworks for Potential Multimodal Imaging

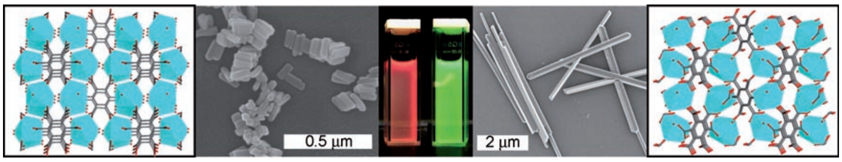

Less basic: By controlling the pH value of the reaction medium, two different gadolinium-containing nanoscale metal–organic frameworks (NMOFs) based on the same building blocks can be synthesized (see picture). The NMOFs carry a large payload of Gd^{3+} centers and are efficient contrast agents for T_2-weighted magnetic resonance imaging. The NMOFs are highly luminescent when doped with other lanthanide ions such as Eu and Tb.

Supramolecular Surface Chemistry

A. Llanes-Pallas, M. Matena, T. Jung,
M. Prato, M. Stöhr,*
D. Bonifazi* ____________ 7726 – 7730

Trimodular Engineering of Linear Supramolecular Miniatures on Ag(111) Surfaces Controlled by Complementary Triple Hydrogen Bonds

Simultaneous three-component assembly on surfaces mediated by triple H-bonding interactions leading to the formation of linear supramolecular miniatures has been studied on Ag(111) surfaces by STM. In particular, the complementary assembly of two linear modules (see picture, blue and green) and an anthracenyl-capped molecular stopper (red) led to the formation of discrete linear oligomeric, pentameric, and trimeric nanoassemblies.

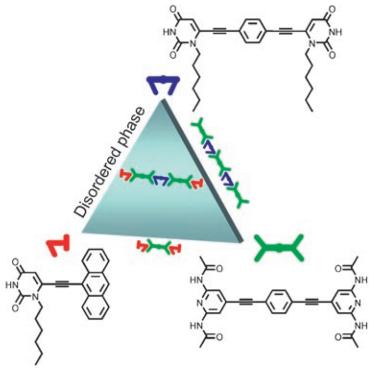

Electrochemiluminescence

C. Booker, X. Wang, S. Haroun, J. Zhou,
M. Jennings, B. L. Pagenkopf,*
Z. Ding* ____________ 7731 – 7735

Tuning of Electrogenerated Silole Chemiluminescence

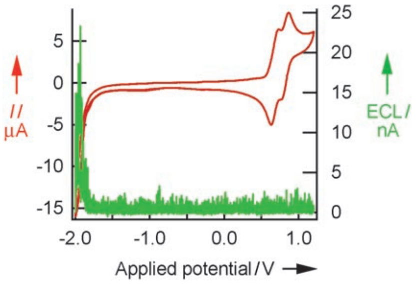

Electrochemical tuning and structural modification of thiophene-substituted siloles led to silole chromophores with efficient and stable electrochemiluminescence (ECL). By extending silole π conjugation with thiophene units and by constraining the applied potential range, stable radical cations favorable for ECL emission were generated (see graph for an example).

Pharmacophore Mapping

J. Orts, J. Tuma, M. Reese, S. K. Grimm,
P. Monecke, S. Bartoschek, A. Schiffer,
K. U. Wendt,* C. Griesinger,*
T. Carlomagno* ______ **7736–7740**

Crystallography-Independent Determination of Ligand Binding Modes

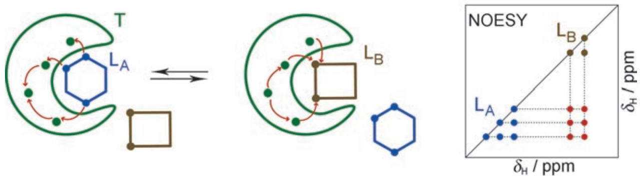

Pass the spin: The internuclear NOE interactions for pharmacophore mapping (INPHARMA) can be used to derive the structure of receptor/ligand complexes for low-affinity lead compounds identified in the early stages of drug discovery. The relative binding mode and, in favorable cases, the absolute binding mode of pairs of competitive low-affinity ligands can be identified with INPHARMA. This is demonstrated for a system comprising protein kinase A (T in the schematic representation) and two activity inhibitors with known structures (L_A and L_B).

Hydrogen Storage

Y.-G. Lee, H. R. Moon, Y. E. Cheon,
M. P. Suh* ______ **7741–7745**

A Comparison of the H_2 Sorption Capacities of Isostructural Metal–Organic Frameworks With and Without Accessible Metal Sites: $[\{Zn_2(abtc)(dmf)_2\}_3]$ and $[\{Cu_2(abtc)(dmf)_2\}_3]$ versus $[\{Cu_2(abtc)\}_3]$

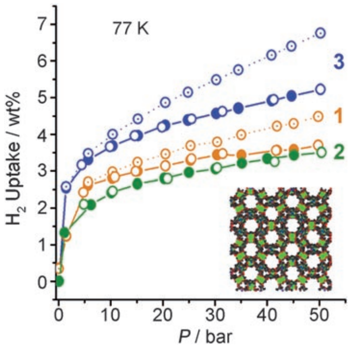

The isostructural metal–organic frameworks $[\{Zn_2(abtc)(dmf)_2\}_3]$ (**1a**), $[\{Cu_2(abtc)(dmf)_2\}_3]$ (**2a**), and $[\{Cu_2(abtc)\}_3]$ (**2b**; $H_4abtc = 1,1'$-azobenzene-3,3',5,5'-tetracarboxylic acid) have high sorption capacities for H_2, N_2, CO_2, and CH_4. Solid **2b**, which has accessible metal sites (AMSs), has a higher H_2 adsorption capacity than **1a** or **2a** (see picture; $T = 77$ K), neither of which have AMSs, because of its lower molecular weight and greater isosteric heat of H_2 adsorption.

Density Functional Calculations

S. N. Pieniazek, F. R. Clemente,
K. N. Houk* ______ **7746–7749**

Sources of Error in DFT Computations of C–C Bond Formation Thermochemistries: $\pi \rightarrow \sigma$ Transformations and Error Cancellation by DFT Methods

Alarming: Multiple sources of errors in DFT energetics of C–C bond-forming reactions were investigated by evaluating structural transformations in Diels–Alder reactions: conversion of π into σ bonds and changes in conjugation, hyperconjugation, and branching interactions. A startling overestimation of the π to σ bond conversion is found with most methods, a central problem to all reactions involving addition of π bonds (electrocyclic processes, ene, aldol).

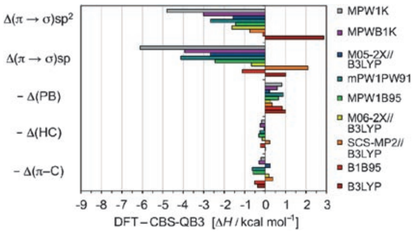

Photomagnetic Nanocomposites

G. Fornasieri, A. Bleuzen* ___ **7750–7752**

Controlled Synthesis of Photomagnetic Nanoparticles of a Prussian Blue Analogue in a Silica Xerogel

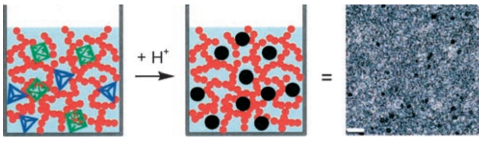

Controlled precipitation: Silica can control the precipitation of a CoFe Prussian Blue analogue (PBA) by reversibly protecting the Co^{II} ions. The precursors are introduced into a silica sol and precipitation of the PBA is triggered by acidification after condensation of the silica network (see picture). This original method provides a homogeneous nanocomposite with important photomagnetic properties.

Fascillating: Inhibitory coupling by bromine among nanoliter aqueous droplets containing the Belousov–Zhabotinsky (BZ) reaction solution produces antiphase oscillations and stationary Turing patterns (see picture; reduced catalyst in red, oxidized catalyst in blue). By choosing the fundamental oscillator and the scavenger added to the connecting medium, it should be possible to construct systems with controllable degrees of inhibitory or excitatory coupling.

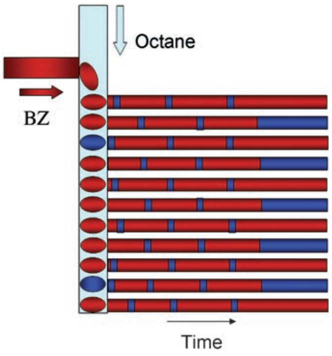

Synchronized Nano-Oscillators

M. Toiya, V. K. Vanag,
I. R. Epstein* ________ **7753 – 7755**

Diffusively Coupled Chemical Oscillators in a Microfluidic Assembly

---

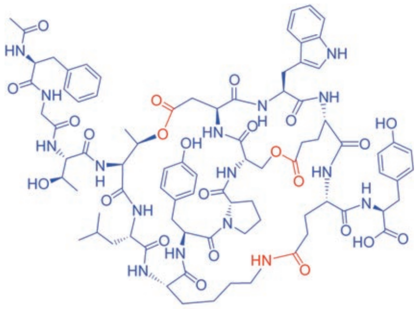

Microviridin B

Decoding biosynthesis: Cage-like depsipeptides have been investigated by a combination of genetic and chemical analyses. Heterologous expression and MALDI-PSD studies reveal that the cyanobacterial protease inhibitors microviridin B and J are synthesized from ribosomally produced prepeptides that are transformed into tricyclic depsipeptides by ATP grasp ligases and processed by a transporter peptidase.

Natural Products

N. Ziemert, K. Ishida, A. Liaimer,
C. Hertweck,* E. Dittmann* **7756 – 7759**

Ribosomal Synthesis of Tricyclic Depsipeptides in Bloom-Forming Cyanobacteria

---

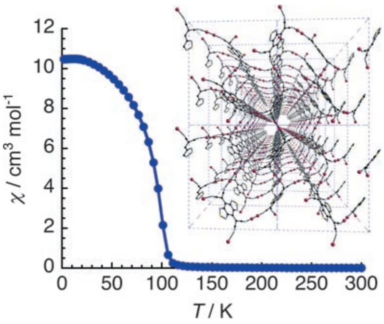

Electron-transfer makes a magnet: 2:1 assembly of $[Ru_2^{II,II}L_4]$ paddlewheel complexes and BDTA-TCNQ yielded a new structural type of electron-transfer system with a three-dimensional network structure which exhibits a long-range ferromagnetic transition at $T_c = 107$ K (see depicted χ vs T curve and inset view of structure along the a axis). L = *m*-fluorobenzoate, BTDA-TCNQ = bis(1,2,5-thiadiazolo)tetracyanoquinodimethane.

Molecule-Based Magnets

N. Motokawa, H. Miyasaka,*
M. Yamashita, K. R. Dunbar **7760 – 7763**

An Electron-Transfer Ferromagnet with $T_c = 107$ K Based on a Three-Dimensional $[Ru_2]_2$/TCNQ System

---

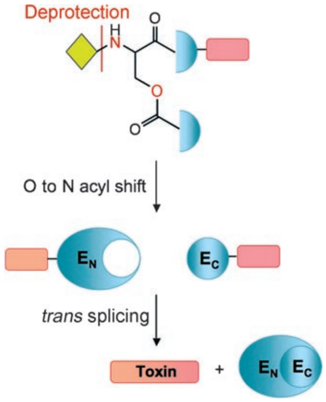

Protein splicing under control: Introduction of an *O*-acyl isomer of a peptide bond into the naturally split *Ssp* DnaE intein prevents protein *trans* splicing, which can be recovered upon triggering an O to N acyl shift by deprotection with protease or light (see scheme). This system allows the splicing of a bacterial toxin to be controlled in response to protease activity.

Protein Splicing

M. Vila-Perelló, Y. Hori, M. Ribó,
T. W. Muir* ________ **7764 – 7767**

Activation of Protein Splicing by Protease- or Light-Triggered O to N Acyl Migration

---

Supporting information is available on www.angewandte.org (see article for access details).

A video clip is available as Supporting Information on www.angewandte.org (see article for access details).

Service

Corrigendum

Nickel-Mediated Coupling Reactions of Carboryne with Alkenes: A Synthetic Route to Alkenylcarboranes

Z. Qiu, Z. Xie* ______ **6572–6575**

Angew. Chem. Int. Ed. **2008**, *47*

DOI 10.1002/anie.200801958

This Communication was published without giving the date of receipt. The correct details for page 6575 (left column, bottom) are given here. The editorial office apologizes for this oversight.

Received: April 25, 2008
Revised: June 6, 2008
Published online: July 30, 2008